NASA TECHNICAL NOTE

NASA TN D-6808

NASA TN D-6808

PREDICTABILITY OF BRAYTON ELECTRIC POWER SYSTEM PERFORMANCE

by John L. Klann and Henry J. Hettel

Lewis Research Center
Cleveland, Ohio 44135

NATIONAL AERONAUTICS AND SPACE ADMINISTRATION • WASHINGTON, D. C. • MAY 1972

1. Report No.	2. Government Accession No.	3. Recipient's Catalog No.
NASA TN D-6808		

4. Title and Subtitle	5. Report Date
PREDICTABILITY OF BRAYTON ELECTRIC POWER SYSTEM PERFORMANCE	May 1972
	6. Performing Organization Code

7. Author(s)	8. Performing Organization Report No.
John L. Klann and Henry J. Hettel	E-6811
	10. Work Unit No. 112-27
9. Performing Organization Name and Address Lewis Research Center National Aeronautics and Space Administration Cleveland, Ohio 44135	11. Contract or Grant No.
	13. Type of Report and Period Covered Technical Note
12. Sponsoring Agency Name and Address National Aeronautics and Space Administration Washington, D. C. 20546	14. Sponsoring Agency Code

15. Supplementary Notes

16. Abstract

Data from the first tests of the 2- to 15-kilowatt space power system in a vacuum chamber were compared with predictions of both a pretest analysis and a modified version of that analysis. The pretest analysis predicted test results with differences of no more than 9 percent of the largest measured value for each quantity. The modified analysis correlated measurements. Differences in conversion efficiency and power output were no greater than ±2.5 percent. This modified analysis was used to project space performance maps for the current test system.

17. Key Words (Suggested by Author(s))	18. Distribution Statement
Brayton 2- to 15-kilowatt system; Electric power system; Analysis; Data comparison; Space power system; Space performance predictions	Unclassified - unlimited

19. Security Classif. (of this report)	20. Security Classif. (of this page)	21. No. of Pages	22. Price*
Unclassified	Unclassified	23	$3.00

* For sale by the National Technical Information Service, Springfield, Virginia 22151

PREDICTABILITY OF BRAYTON ELECTRIC POWER SYSTEM PERFORMANCE

by John L. Klann and Henry J. Hettel

Lewis Research Center

SUMMARY

Data from the first tests of a 2- to 15-kilowatt Brayton space electric power system in a vacuum chamber were compared with analytical predictions of its steady-state performance. Comparisons were limited to results from one of two sets of identical turbomachinery that were used in the tests, and to the design helium-xenon working gas mixture. Differences between analytical values and measurements were expressed in percent of the largest measured value for each quantity.

The pretest analytical values for conversion efficiency and power output were higher than the measurements. Differences were no more than +9 percent for conversion efficiency and +6 percent for power output. Refinements of the pretest analysis were made. This modified analysis correlated conversion efficiency and power output. Differences were no greater than ±2.5 percent in efficiency and ±2.0 percent in power.

The modified analysis was used to project space performance maps for the current test system. These maps show the trade-off among thermal power needs, required radiator area, and net electric power output.

INTRODUCTION

The ability to analytically predict system performance is a useful research tool. Such a tool was developed as part of the NASA technology program on Brayton-cycle space power systems. The analysis is presented in reference 1. Although it was made specifically for the 2- to 15-kilowatt Brayton power system, the methods can be used for other closed-Brayton-cycle systems.

The analysis synthesized the system and was used in a digital computer program. Both component test results and design values were used. However, the analysis was made before any system tests. And, in reference 1, the predicted system efficiencies were reduced by 20 percent to allow for neglected effects. The analysis has been used

to size test-support equipment, to evaluate potential system changes, and to make initial application studies.

Within the overall program on the 2- to 15-kilowatt system, Lewis Research Center has completed its first system tests in a vacuum chamber. Vernon and Miller (ref. 2) present the test results. Reference 3 describes the overall program status. The current test system is capable of useful outputs up to 10.5 kilowatts. Reference 3 shows that with minor improvements the system should be capable of useful outputs in the range of 2 to 15 kilowatts.

The major purpose of this investigation is to check the importance of neglected effects in the pretest analysis. A secondary purpose is to project the best estimates of the current power system's performance in space.

The analytical results of reference 1 are compared with measurements presented in reference 2. Based on the system test measurements, the pretest analysis was refined to include a system heat-loss term. Further comparisons are made between the modified analysis and test measurements. The more accurate modified analysis is then used to generate space performance maps for the current system.

TEST CONFIGURATION

In the power system test setup, support equipment was used to simulate a space-type heat source and radiator. A radiant electric heater was used in place of a radioisotope heat source. An auxiliary heat exchanger, cooled by a facility refrigeration system, was used in place of a space-type radiator. The power-system test configuration is shown schematically in figure 1. The power-conversion module includes everything except the heat-source subsystem and the radiator-simulator heat exchanger. The closed gas loop includes the heat-source heat exchanger and the ducting to and from the power-conversion module.

The closed gas loop is recuperated. The design working gas is a helium and xenon mixture with the molecular weight of krypton, 83.8. A turbine, alternator, and compressor are assembled on a single shaft. During operation, the electrical subsystem controls the shaft speed to about 3770 rad/sec (36 000 rpm); the shaft is supported by self-acting gas bearings. Design gas temperatures are 1144 K (1600° F) at the turbine inlet and 300 K (80° F) at the compressor inlet. The design compressor-outlet operating pressure range is from about 10 to 30 N/cm^2 (15 to 45 psia).

The gas management subsystem supplies working gas to the closed loop and allows changes in gas loop pressures. The electrical subsystem, in addition to controlling machinery speed, also regulates output voltage and distributes output power. Alternator output is split among a user-load bus, a parasitic-load resistor, and a dc power supply

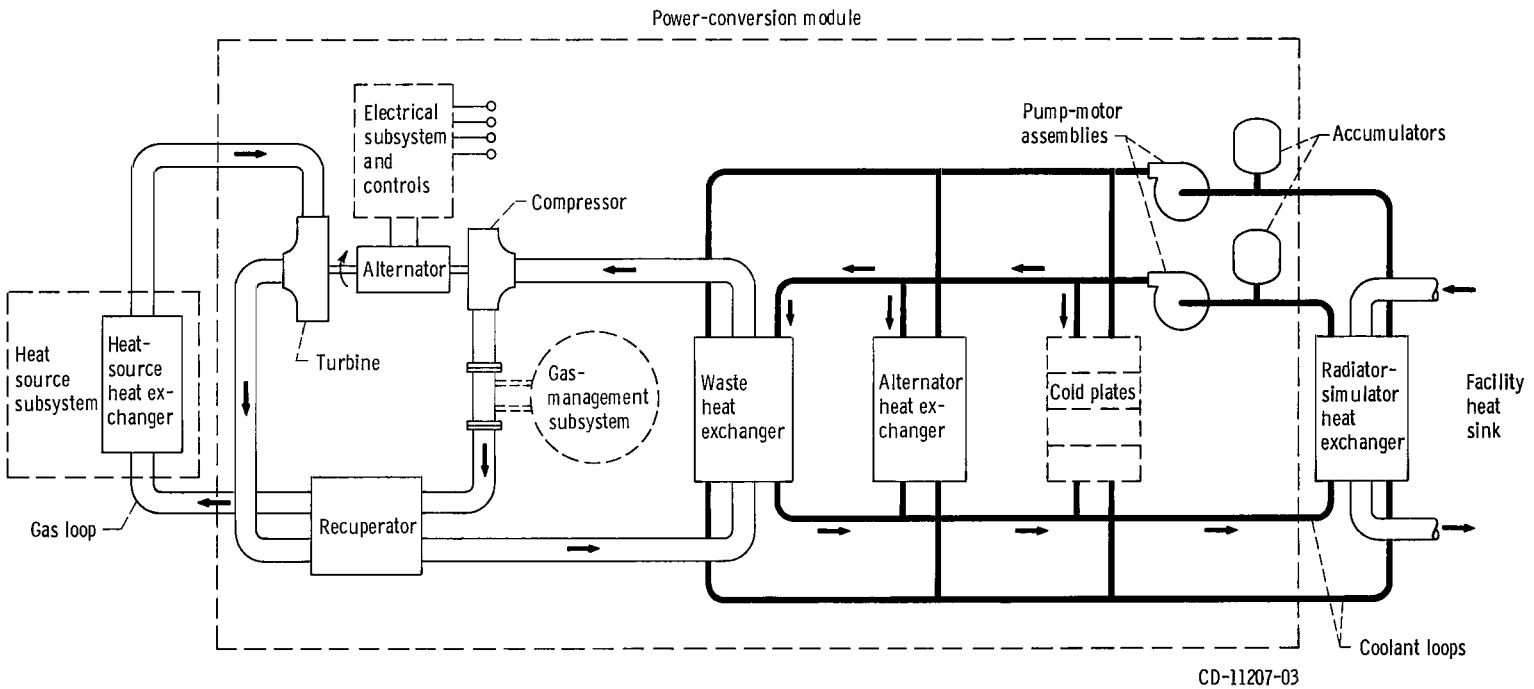

Figure 1. - Schematic diagram of power-system test configuration.

for system housekeeping power. The power at the user bus is 3-phase at 1200 hertz and 120 volts, line to neutral.

The power-system coolant is a silicone oil. There are dual coolant loops; however, only one operating cooling loop is needed. Each loop has three parallel paths through the waste heat exchanger, a set of alternator cooling coils, and a series of cold plates for electrical subsystem component cooling.

Figure 2 is a photograph of the test system installed in the vacuum chamber. The power-conversion module was made up of compactly arranged, flight-type components.

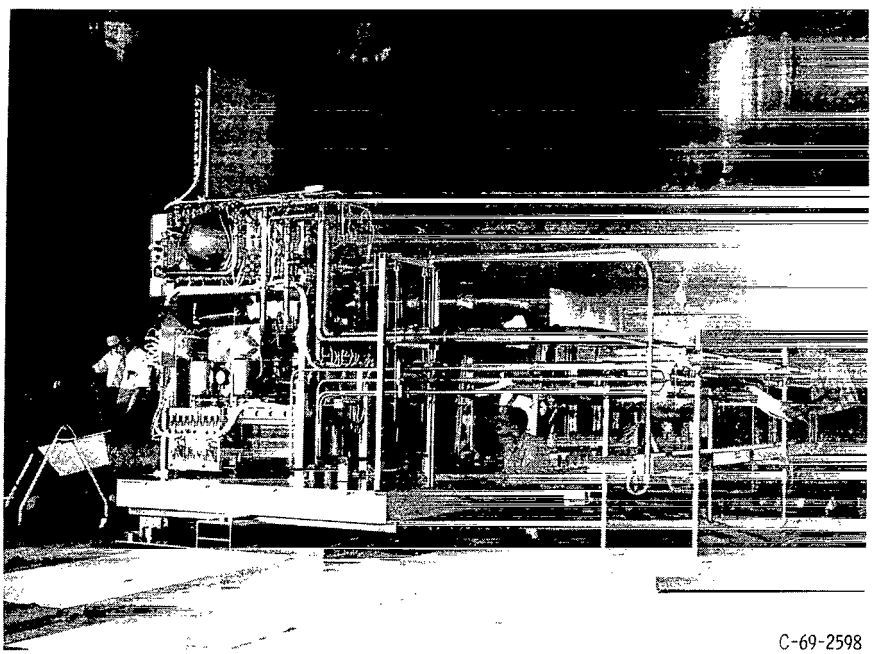

C-69-2598

Figure 2. - Brayton test system installed in vacuum chamber.

Components of the module were mounted in and around the rectangular frame that is visible in the left foreground of figure 2. The frame measures 0.8 by 1.4 by 2.3 meters (33 by 55 by 90 in.). The power-conversion module contained all of the equipment needed for its independent operation.

INSTRUMENTATION AND MEASUREMENTS

In this test, the amount of instrumentation was limited to obtain only overall system performance and gross component performance. The test measurements used for comparisons between experimental and analytical data are shown in table I. Gas-loop tem-

TABLE I. - LOCATION, TYPE, AND NUMBER OF TEST MEASUREMENTS USED IN COMPARISONS

Location	Type	Number
Turbine inlet	Temperature	3
	Wall static pressure	2
Turbine outlet	Wall static pressure	1
Recuperator hot-side inlet	Temperature	3
Transition between recuperator and waste-heat exchanger	Temperature	4
Waste heat exchanger outlet	Temperature	3
Compressor inlet	Wall static pressure	1
Compressor outlet	Wall static pressure	1
Recuperator cold-side inlet	Temperature	3
Recuperator cold-side outlet	Temperature	2
Duct from recuperator to source heat exchanger	Static-pressure change	2
Turbomachinery shaft	Rotational speed	2
Alternator output terminals	Power	1

perature measurements were made with probe thermocouples. Pressure measurements were made with wall taps connected to strain-gage transducers. A small correction was applied to these static measurements to obtain total pressures (ref. 2). Gas mass-flow rate was obtained from the measured static-pressure change in a high-recovery venturi-type meter. This meter was located in a straight section of the duct from the recuperator to the heat-source heat exchanger. Turbomachinery speed was measured by magnetic probes. The three-phase, gross power output of the alternator was measured with a high-frequency quarter-square multiplier.

Table II shows a summary of the measured ranges in steady-state data. The power system was operated for a total of 2561 hours by using two sets of identical turbomachinery. The first set was replaced after a failure at 668 hours. Cause of the failure was corrected and the second set of turbomachinery was used to a planned shutdown. Both the design helium-xenon mixture and krypton were used.

The longest operating time and the most complete mapping was obtained with the second set of turbomachinery and the helium-xenon mixture. This was also the only combination that was tested at the design turbine-inlet temperature. Emphasis was placed on the high-power-output range (or high-pressure range), and no attempt was made to test below a compressor-outlet pressure of about 17 N/cm^2 (25 psia). The lower design pressure range, down to about 10 N/cm^2 (15 psia), has been studied in a separate atmospheric test of the gas loop. Preliminary results of the atmospheric test were reported in reference 4.

Temperatures and pressures were averaged where there were more than one measurement (table I). At those stations with 3 or 4 thermocouple probes, the spread in

TABLE II. - SUMMARY OF TEST TIMES AND MEASURED STEADY-STATE DATA

Turbo-machinery	Working gas	Test time, hr	Turbine-inlet temperature, K (^{o}F) (a)	Compressor-inlet temperature, K (^{o}F) (b)	Compressor-outlet pressure, N/cm^2 abs (psia) (c)
First set	Helium-xenon mixture	84	1030 to 1090 (1400 to 1500)	300 (80)	17 to 31 (25 to 45)
	Krypton	584	1030 (1400)	300 (80)	17 to 31 (25 to 45)
Second set	Helium-xenon mixture	1535	980 to 1140 (1300 to 1600)	300 (80)	17 to 31 (25 to 45)
				280 to 310 (40 to 90)	24 (35)
	Krypton	358	980 to 1090 (1300 to 1500)	300 (80)	17 to 24 (25 to 35)
			1030 to 1090 (1400 to 1500)	280 to 310 (50 to 90)	24 (35)

[a]Temperature ranges measured in increments of 60 K (100^{o} F).
[b]Temperature ranges measured in increments of 6 K (10^{o} F).
[c]Pressure ranges measured in increments of 3 N/cm^2 (5 psi).

TABLE III. - IDEAL-MEASUREMENT PROBABLE ERRORS

(a) Direct measurements

Measurement	Relative probable error, percent
Alternator gross power	±1.0
Temperature	±.4
Static pressure	±.2

(b) Indirect measurements

Measurement	Relative probable error, percent
Gross conversion efficiency	±1.5
Turbine temperature drop	±1.2
Thermal input to power-conversion module	±1.1
Gas mass-flow rate	±.5
Gas waste heat load	±.5
Recuperator heat-transfer effectiveness	±.4
Compressor temperature rise	±.3
Compressor pressure ratio	±.3
Turbine pressure ratio	±.2
Average turbine-inlet temperature	±.2
Average compressor-inlet temperature	±.2

temperature was from 2 to 3 K (3° to 6° F). Dual pressure measurements were within 0.1 N/cm^2 (0.1 psia) of each other.

Ideal measurement probable errors are listed in table III. The manufacturer's specified error band of a single sensor is shown in table III(a). The calculated probable errors of the indirect measurements (table III(b)) are based on the errors listed in table III(a). The calculated errors are ideal, or minimum, values. They neglect other sources of possible error, such as those due to signal conditioning and data recording. The minimum errors are presented as a guide in comparing data with theory.

Among the indirect measurements, gross conversion efficiency has the largest ideal probable error, ±1.5 percent. Gross conversion efficiency is defined as the power at the alternator terminals, or alternator gross power output, divided by the thermal power input to the power-conversion-module working gas. Mathematically, this thermal power input is the product of the gas mass-flow rate, the gas specific heat at constant pressure, and the temperature difference between the turbine inlet and the recuperator cold-side outlet. Gross conversion efficiency neglects both heat-source thermal losses and system housekeeping power needs.

There is an added uncertainty in the accuracy of the high-temperature gas-loop measurements (i.e., those at the turbine-inlet, turbine-outlet, and recuperator "cold-side" outlet). This is because of a radiation error in the measurements which would be important only at high-temperature stations. All temperature probes were polished before the tests. Post-test inspection showed discoloration. The darkening of the probes would increase their radiation heat losses. This would cause the sensed temperature to be lower than the actual gas temperature.

Thermocouple corrections are based on a balance between the convective heat transfer from the gas to the probe and the radiation and conduction heat losses from the probe. The thermal conductivity of the helium-xenon mixture is about 2.5 times that of krypton. Therefore, the convective heat transfer coefficient for the mixture is larger than that for krypton. With the same radiation and conduction heat losses, the temperature corrections for krypton would be larger than those for the gas mixture.

There was one duct-wall temperature measurement at the turbine-inlet station. The difference between the sensed gas temperature and that at the wall varied from about 10 to 30 K (25° to 50° F) for both gases. However, because of the limited measurements, no consistent correction can be made. The authors conjecture that the high-temperature (900- to 1140-K (1200°- to 1600°-F)) measurement corrections are of the order of +5 K ($+10^{\circ}$ F) for the mixture data, and of the order of +30 K ($+50^{\circ}$ F) for the krypton data. The data presented in this report are uncorrected.

METHOD OF ANALYSIS

Details of the pretest analysis are presented in reference 1. The analysis was approximate since it neglected thermal losses from the system and the effects of any flow maldistributions due to ducting between components. The power-system synthesis was based on a combination of design values and component test results. Turbine and compressor performance maps used were obtained in separate tests of each component (refs. 5 and 6). Results of test data (ref. 7) for alternator electromagnetic efficiency were also used. The recuperator and waste heat exchanger heat-transfer analytical models were modified to reflect the results of acceptance tests on those components. Heat exchanger and ducting gas pressure drops were based on design predictions. Also, all turbomachinery shaft losses - bearing friction, alternator windage, and bleed-flow losses through shaft seals - were obtained from design predictions.

Modified Analysis

The pretest analysis was refined to include a heat-loss term. This term accounts for heat losses from the power conversion module. In the modified analysis, the loss was added to the ideal power-conversion-module thermal input. The size of the heat loss was based on measurements from the tests in the vacuum chamber.

The alternator coolant heat load consists of the sum of losses from electromagnetic inefficiency, shaft windage, bearing friction, and conduction (mainly from the hot turbine). Over the output power range, the measured alternator-coolant heat load was from 0.7 to 0.8 kilowatt larger than the sum of predicted losses that did not include the conduction loss. Therefore, the conduction loss was assumed to be about 0.7 kilowatt. Radiation heat losses from the insulated power-conversion module are estimated to be about 0.5 kilowatt. Hence, 1.2 kilowatts, the sum of these two previously unaccounted losses, was used for the heat-loss term.

In addition to the neglected heat losses in the pretest analysis, there also were differences between the assumed analytical conditions and the test conditions. Some of these differences were accounted for in the modified analysis. Table IV lists the differences among the assumed conditions for the pretest and the modified analyses and the test conditions. The changes in assumed conditions for the modified analysis include turbomachinery speed, alternator load power factor, and heat-exchanger pressure drops.

The pretest analysis assumed the design turbomachinery speed of 3770 rad/sec (36 000 rpm). The test results show that the average speed for the second set of turbomachinery was about 3790 rad/sec (36 200 rpm). The shaft speed is a function of the control system and varies somewhat with the amount of power dissipated in the parasitic

TABLE IV. - DIFFERENCES AMONG ASSUMED ANALYTICAL CONDITIONS AND TEST CONDITIONS

	Pretest analysis	Modified analysis	Test conditions
Heat losses, kWt	0	1.2	1.2
Turbomachinery speed, rad/sec (rpm)	3770 (36 000)	3790 (36 200)	3790 (36 200)
Alternator load power factor	0.75	1.0	1.0
Heat exchanger pressure drops, percent			
Heat-source heat exchanger	2.2	3.2	3.2
Recuperator hot side	2.2	1.8	1.8
Recuperator cold side	1.1	.8	.8
Waste heat exchanger	.73	1.6	1.6
Turbomachinery axial clearances, cm (in.)			
Turbine	0.025 (0.010)	0.025	0.050 (0.070)
Compressor	.020 (0.008)	.020	.038 (0.015)
Compressor-inlet duct	Straight	Straight	90° Elbow
Bleed mass-flow rate, percent	2	2	Probably less than 2

load (ref. 8). A speed of 3790 rad/sec was used in the modified analysis. Also, reference 1 used the alternator efficiency for the design alternator load power factor of 0.75, lagging. Almost all of the alternator load during the test was resistive and resulted in a power factor of about 1.0. The modified analysis assumed the higher alternator efficiency for a power factor of 1.0. The resulting increase in gross alternator power is about 100 watts.

Heat exchanger pressure drops were changed on the basis of the measured results. The pressure drops in table IV are expressed in terms of percent of the component's inlet pressure. The measured recuperator pressure drops were lower, while both the waste heat exchanger and heat-source heat exchanger pressure drops were higher. This overall effect on system output was small.

Other differences between the conditions assumed for the analyses and the test conditions (table IV) include differences in turbomachinery axial clearances, the compressor-inlet duct, and bleed mass-flow rate. Their effects are small and remain

neglected. The turbine and compressor maps used in the analyses were obtained with design values of axial clearance between the rotors and their shrouds. In the vacuum-chamber test, these clearances were roughly doubled. Component tests on the effects of axial clearance showed small reductions in mass-flow rate and efficiency with doubled clearances. Clearance effects on the turbine were reported in reference 9. The compressor results are not yet published.

Another neglected difference is that the compressor maps used in the analyses were obtained with a straight inlet duct, while the system configuration uses a 90° elbow just upstream of the compressor. Compressor component tests with the 90° elbow showed a 0.02 reduction in peak efficiency. However, at the system operating corrected mass-flow rate, which is off peak efficiency, there was no efficiency loss. These component results remain to be published.

Part of the compressor-outlet flow is ducted to the turbomachinery shaft cavities to provide the ambient pressure for the self-acting gas bearings. This flow reenters the gas loop because of leakage through both the turbine- and compressor-end labyrinth shaft seals. In the analyses, the design value of bleed mass-flow rate was assumed. In the system tests, this flow was not measured. However, in a separate test (ref. 10) of the turbomachinery, the measured bleed-flow rate was 1.2 percent. Effects of this difference are small and remain neglected.

Space Performance

The modified analysis was used to generate space performance maps for the current Brayton power system. For these calculations only, an alternator load power factor of 0.85 was used. The split radiator configuration of reference 11 was assumed to be a logical arrangement for space flight. This arrangement is shown in figure 3. The

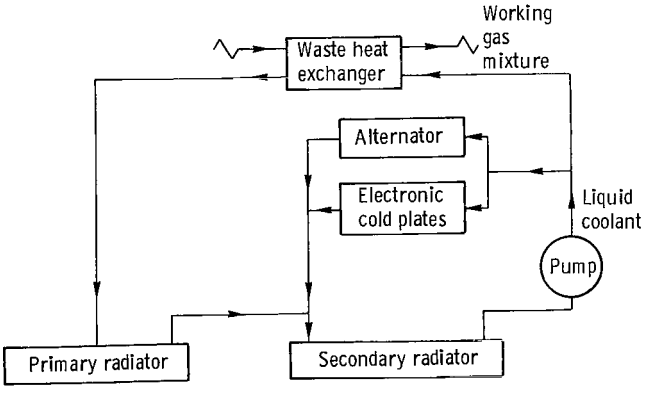

Figure 3. - Radiator and cooling-loop arrangement.

pumped coolant flow is split among the primary heat load from the waste heat exchanger and the secondary heat loads from the alternator and the electronic coldplates. All of the coolant flow passes through the secondary radiator, while only part of the coolant flows through the primary radiator. The primary radiator is sized such that its outlet temperature equals the mixed outlet temperature from the secondary heat loads.

The secondary heat loads used in these calculations were based on measured values from the system tests in vacuum. Figure 4 shows the alternator cooling load plotted against alternator gross power output. Data are shown for the measured range of turbine-inlet temperature and two values of coolant mass-flow rate. Within the data scatter, the cooling load was a linear function of gross output. The calculations assumed the straight line shown in figure 4. Coolant mass-flow rate was not allowed to be less than 0.068 kg/sec, the lowest tested value. And coolant temperature rise was not allowed to exceed 14 K (25^{o} F).

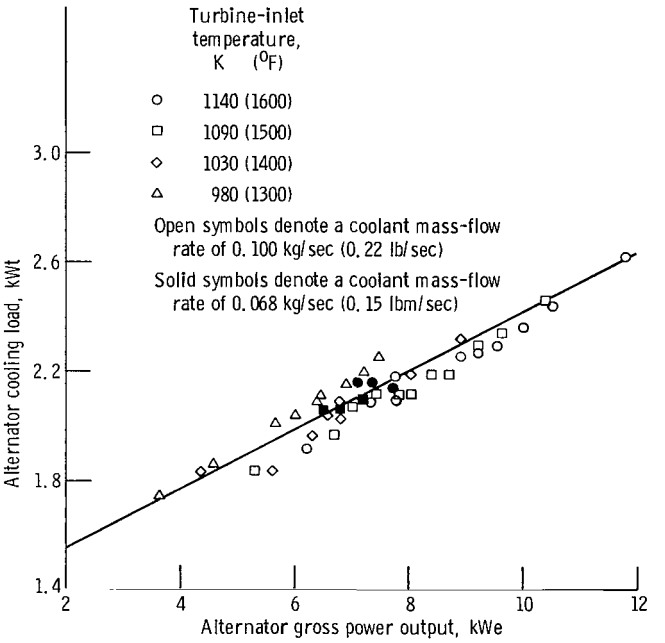

Figure 4. - Measured alternator cooling loads.

Figure 5 shows the measured cold-plate cooling load as a function of the coolant-inlet temperature. Only one value of coolant mass-flow rate was used in the tests. Reference 8 shows that the thermal losses from the electronic components were approximately constant and independent of alternator gross power. The lines through the data show an average heat load of about 1 kilowatt for inlet temperatures up to about 295 K (70^{o} F). The decrease in measured heat load above 295 K indicates insufficient cold-

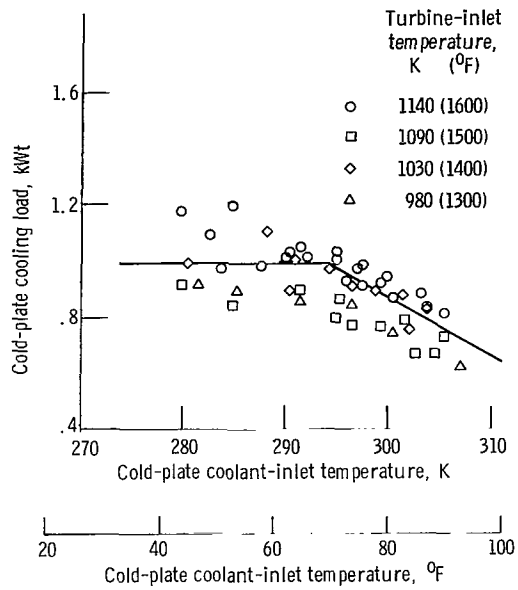

Figure 5. - Measured cold-plate cooling loads. Coolant mass-flow rate, 0.03 kg/sec (0.07 lbm/sec).

plate cooling and an increase in radiation heat loss from the electronic components. In the space performance calculations, the cold-plate heat load was assumed to be 1 kilowatt. Coolant mass-flow rate was not allowed to be less than 0.03 kg/sec. And coolant temperature rise was not allowed to exceed 19 K (34° F).

Because of operational lifetime temperature limits on the current electronic components, the cold-plate coolant inlet temperature was not allowed to exceed 311 K (100° F). Therefore, in the space performance calculations, the coolant pump-outlet temperature was restricted to 311 K or less.

System prime radiator areas were calculated (ref. 1) within the constraints of the secondary heat loads and for a range in equivalent heat-sink temperatures. A radiator surface hemispherical emittance of 0.9 was assumed. Radiator equivalent heat-sink temperature is a function of position and orientation in space. It is defined as the equilibrium temperature for a small element of radiator surface when it is not rejecting heat. Prime radiator area assumes that waste heat is rejected at the coolant bulk temperature to the equivalent heat-sink temperature. Axial temperature changes in the direction of the coolant flow are accounted for; while the effects of both coolant-to-tube and lateral, tube-to-fin temperature drops are neglected. Detailed radiator analyses have shown that actual areas, 17- to 23-percent greater than prime area, result in radiator weights that are 10 percent above the smallest possible radiator weights. In this study, prime radiator areas were increased by 20 percent to approximate realistic area needs.

For the space performance calculations, system net power output is defined as the alternator gross power output minus 1.4 kilowatts. Reference 8 shows that 1.15 kilo-

watts of power are needed for the electrical components over their operational range. An estimate of the minimum residual power needed in the parasitic load for stable speed control operation is 0.25 kilowatt. Hence, the 1.4 kilowatts represents a minimum value of system housekeeping power needs.

RESULTS AND DISCUSSION

Both component and overall power-conversion module performance are compared with analytical predictions. Overall performance for a constant set of gas pressures and temperatures is given by alternator gross power output and gross conversion efficiency. Component performance includes turbomachinery parameters and heat-exchanger parameters. Differences between analytical values and measurements are expressed in percent of the largest measured value for each quantity.

Comparisons are limited to the test results obtained with the second set of turbomachinery and the helium-xenon gas mixture. Test data for krypton were not used because of thermocouple radiation errors and insufficient measurements for a satisfactory correction. Data obtained with the first set of turbomachinery showed about 8 percent less alternator gross power output than that obtained with the second set at the same apparent operating conditions. Because of uncertainties in exact test conditions, the lower performance with the first set of turbomachinery is unexplained. Lower levels of compressor and turbine pressure ratio were measured with the first set of turbomachinery. The lower levels in pressure ratio might be due to turbomachinery shaft operation at the low side of the speed control-band. However, no accurate measure of shaft speed was obtained during this part of the test.

Comparison With Pretest Analysis

Figure 6 shows a comparison between test data and the pretest analysis. Effects of compressor-outlet pressure and turbine-inlet temperature on performance are shown. Compressor-inlet temperature is about 300 K. In the figure, the symbols represent experimental data, and the lines represent the analytical predictions. Figure 6(a) shows overall performance; figure 6(b), turbomachinery performance; and figure 6(c), heat-exchanger performance.

Comparisons showed that the largest percent differences occurred in gross conversion efficiency. As expected because of the omission of heat losses in the pretest analysis, the data were lower than the predictions. The largest absolute difference was 0.03, which, compared with the highest measured efficiency (0.325), results in a +9 percent

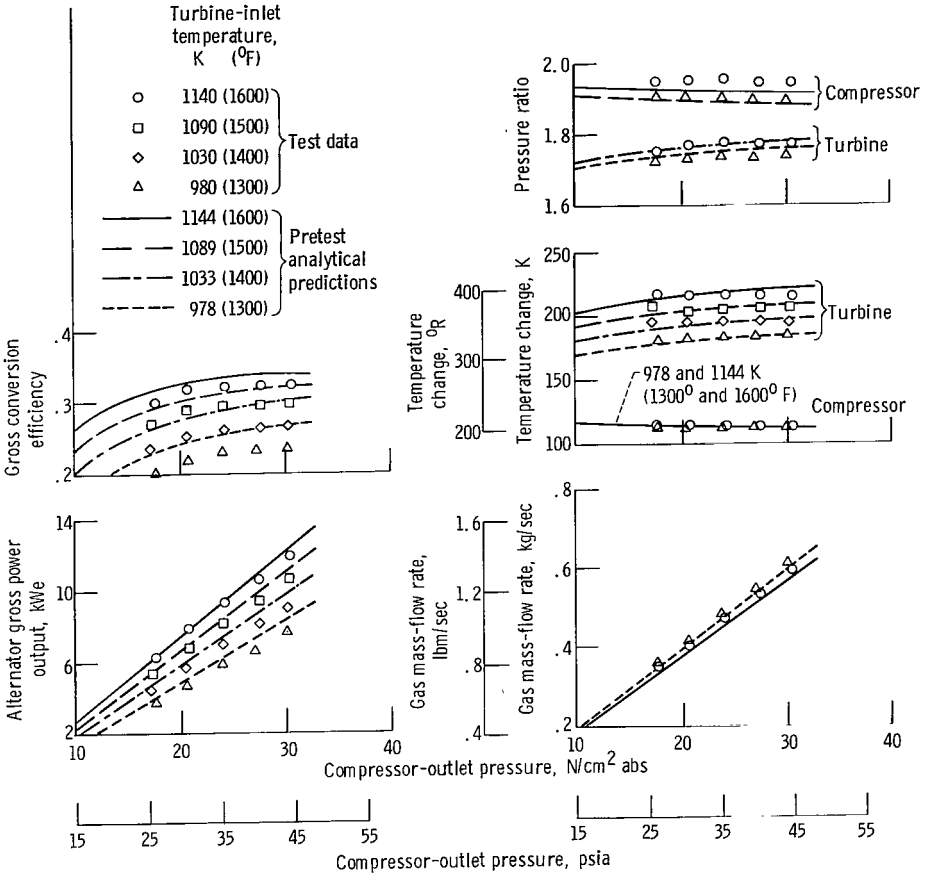

(a) Overall performance.

(b) Turbomachinery performance.

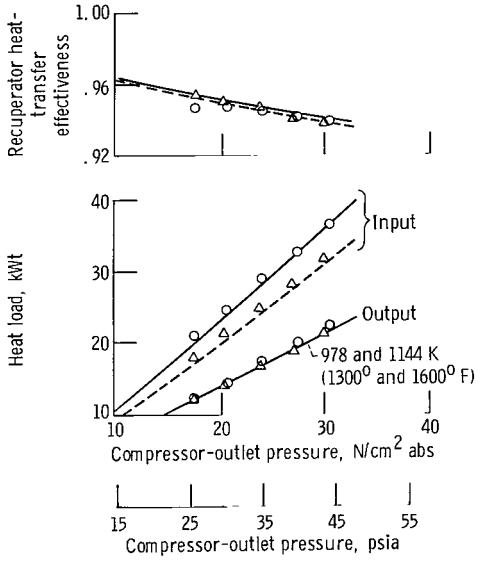

(c) Heat-exchanger performance.

Figure 6. - Comparison of test data with pretest analytical predictions of the effects of compressor-outlet pressure and turbine-inlet temperature on performance. Compressor-inlet temperature, 300 K (80° F).

difference. Hence, the 20 percent allowance for neglected effects in reference 1 was conservative.

Alternator gross power output measurements (fig. 6(a)) were also lower than the predictions. The largest difference was 0.7 kilowatt, or +6 percent of 11.85 kilowatts, the largest measured value.

Analytical component performance parameters (figs. 6(b) and (c)) differed by no more than 3 percent from the measurements. In figure 6(b), gas mass-flow rate and the temperature changes and pressure ratios across the turbine and compressor are plotted against compressor-outlet pressure. The analytical mass-flow rates were about 0.02 kg/sec (0.04 lbm/sec) lower than the measured values. Magnitudes of the compressor temperature rise and the turbine temperature drop were in agreement with predictions. However, the data showed an essentially constant turbine temperature drop at each inlet-temperature level. Predicted compressor pressure ratios were low by about 0.03 at a turbine-inlet temperature of about 1140 K and by about 0.01 at 980 K. Turbine pressure ratios were in agreement at about 1140 K, while at 980 K the predicted turbine pressure ratios were high by about 0.02.

In figure 6(c), the heat input to and the heat output from the power-conversion module working gas and the recuperator heat-transfer effectiveness are plotted against compressor-outlet pressure. Predicted heat input was low by about 1 kilowatt. The measured heat from the gas in the waste heat exchanger correlated with the analysis. System waste heat output was nearly independent of turbine-inlet temperature. Similarly, there was very little effect of turbine-inlet temperature on recuperator heat-transfer effectiveness. The changes in effectiveness with pressure level were in good agreement. The largest difference was +0.007.

These results show that the pretest analysis differed by no more than 9 percent from the largest measured value for each quantity. The combination of neglected effects and minor differences between assumed analytical and test conditions were not of major importance, and judgements made on the basis of the pretest analysis were valid.

Comparison With Modified Analysis

Figure 7 repeats the format and data of figure 6. However, the lines in figure 7 represent the results of the modified analysis. In general, the modifications brought the analytical results and the test data into closer agreement. Gross conversion efficiency and alternator gross power output were correlated. Differences were no greater than ±2.5 percent in power output. The improved efficiency agreement was mainly because of the 1.2-kilowatt heat loss added to the analysis. Better agreement in power output and compressor pressure ratio (fig. 7(b)) was obtained mainly because of the small increase in shaft speed over that used in the pretest analysis.

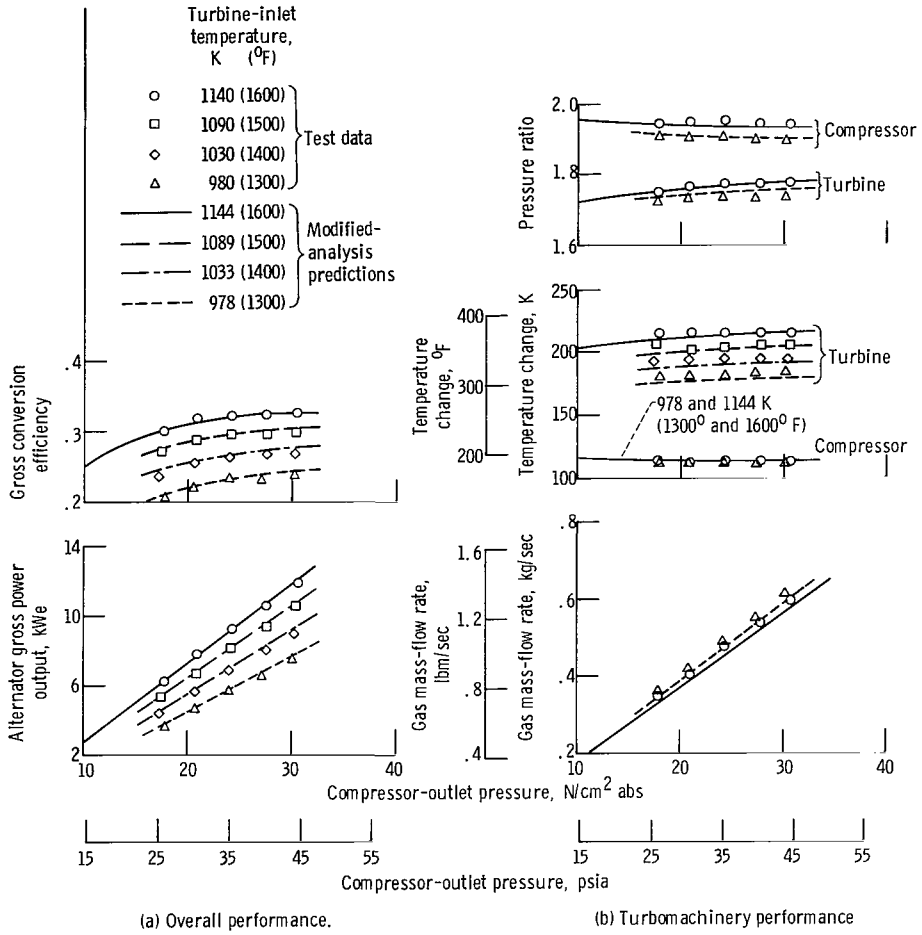

(a) Overall performance.

(b) Turbomachinery performance

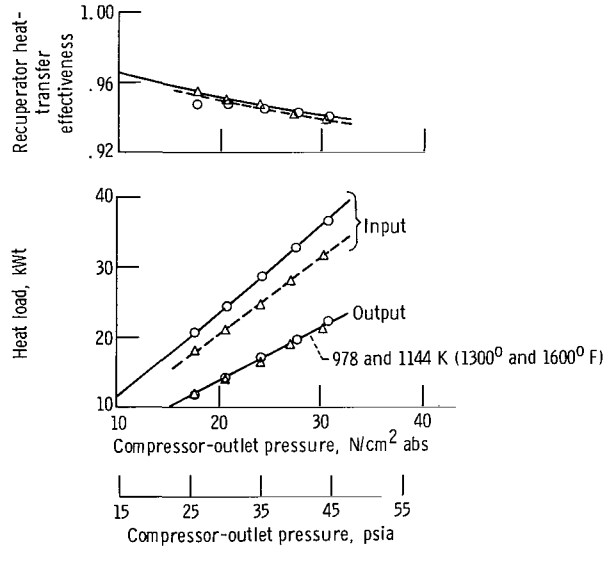

(c) Heat-exchanger performance.

Figure 7. - Comparison of test data with modified-analysis predictions of the effects of compressor-outlet pressure and turbine-inlet temperature on performance. Compressor-inlet temperature, 300 K (80° F).

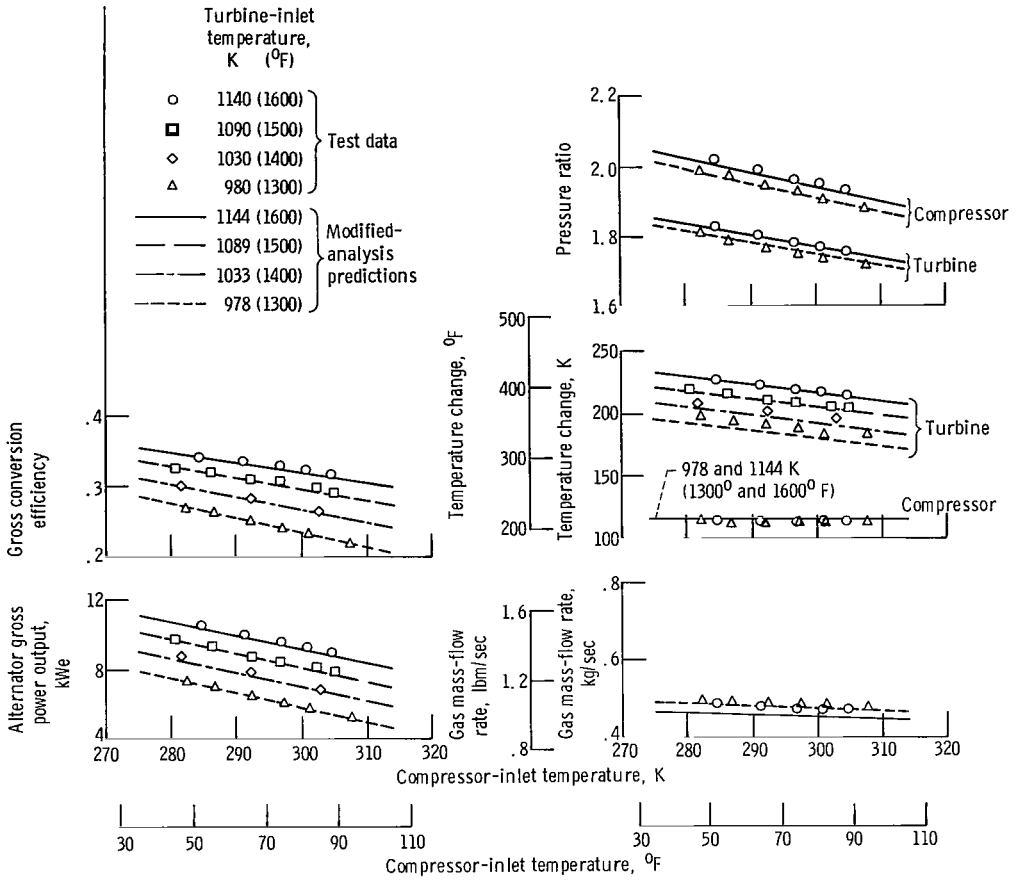

(a) Overall performance.

(b) Turbomachinery performance.

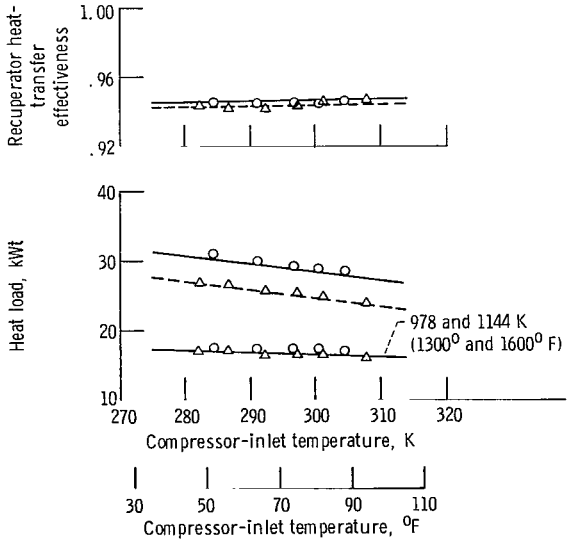

(c) Heat-exchanger performance.

Figure 8. - Comparison of test data with modified-analysis predictions of the effects of compressor-inlet and turbine-inlet temperatures on performance. Compressor-outlet pressure, 24 N/cm^2 abs (35 psia).

A further comparison between test data and the modified analysis is shown in figure 8. Here the abscissa is compressor-inlet temperature. Compressor-outlet pressure is about 24 N/cm^2. Good correlation occurred. Differences in conversion efficiency and power output were within ±2.0 percent. Remaining differences, particularly in turbomachinery performance, shown in figures 7(b) and 8(b), are probably due to a combination of the neglected small effects in the analyses and the limited number of measurements.

The modified analysis predicted measured power output and conversion efficiency with differences of no more than ±2.5 percent. Although the comparisons were limited to the data obtained with one set of turbomachinery and the helium-xenon mixture, the authors believe that the modified analysis can be used to accurately project current power system performance in user application studies.

SPACE PERFORMANCE MAPS

The modified analysis was used to project current power conversion module performance in space applications. Figure 9 shows performance maps for the design turbine-inlet temperature of 1144 K. The assumed equivalent radiator heat sink temperature was 222 K for figure 9(a), 250 K for figure 9(b), and 278 K for figure 9(c). System net power output is plotted against radiator area. On each map, dashed curves are used to show constant levels of thermal input to the power-conversion module. Solid curves show the design extremes of compressor outlet pressure, about 10 and 30 N/cm^2. These pressure extremes are assumed to be the limiting operational values for the current hardware (ref. 1). Also, solid curves are cross-plotted on the results to indicate values of compressor-inlet temperature.

These maps show the tradeoff available among thermal power needs, required radiator area, and electric net output. A user would select the map for the highest value of equivalent radiator heat-sink temperature that is expected for his application. Then for a minimum desired net electric output, he could tradeoff size, weight, and cost of a heat-source against that of a radiator. Since these maps neglect heat-source thermal losses, the user would need to account for them in his source sizing procedure.

Heat-source size is a function of the thermal power input or net conversion efficiency (the ratio of net output to power-conversion-module thermal input). Net conversion efficiency increases with increasing gas pressure and decreasing compressor-inlet temperature. The highest operational efficiencies at each value of compressor-inlet temperature occur at a compressor-outlet pressure of 31.0 N/cm^2. Net conversion efficiencies implied in figure 9 at a pressure of 31.0 N/cm^2 increase from 0.23 at a temperature of 333 K and approach 0.32 at temperatures near 267 K. Similarly, the lowest

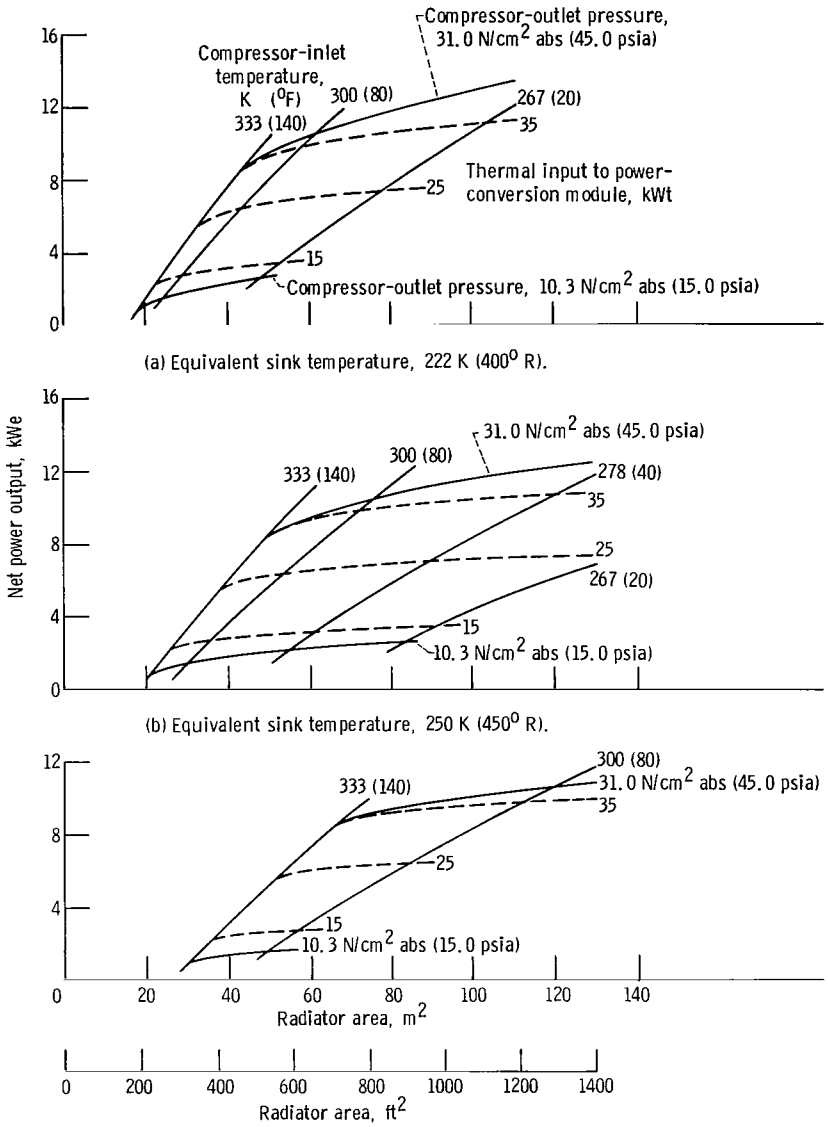

Figure 9. - Space performance maps. Design turbine-inlet temperature, 1144 K (1600° F); radiator emissivity, 0.90; alternator load power factor, 0.85.

efficiencies at each value of compressor-inlet temperature occur at a compressor-outlet pressure of 10.3 N/cm^2. Net conversion efficiencies at 10.3 N/cm^2 increase from 0.05 at 333 K to 0.20 at 267 K.

Although conversion efficiency is improved, operation at low values of compressor-inlet temperature, compared with the expected heat-sink temperature, is not likely for

most applications because of the large radiator area needs. Specific radiator area, the ratio of radiator area to net electric output, is a measure of relative heat rejection needs. Specific radiator needs decrease with decreasing equivalent heat-sink temperature and increasing compressor-inlet temperature and gas pressure. The lowest specific radiator areas in figure 9, over the operational pressure range and at each value of heat-sink temperature, occur at a compressor-inlet temperature of about 333 K. Further increases in compressor-inlet temperature result in small decreases in area and still lower efficiencies. For each map on figure 9, minimum values of specific radiator areas occur at 31.0 N/cm^2 and 333 K. At these conditions, the net electric output is 8.4 kilowatts. For a sink temperature of 222 K, the minimum specific radiator area is about 5.1 m^2/kWe (55 ft^2/kWe); at 250 K, about 5.8 m^2/kWe (63 ft^2/kWe); and at 278 K, about 7.8 m^2/kWe (84 ft^2/kWe).

The shapes of the performance maps above a compressor-inlet temperature of about 320 K (110° F) are slightly influenced by the assumed coolant-loop arrangement (fig. 3) and the cold-plate coolant-inlet temperature limit of 311 K. The optimum (or minimum-radiator-area condition, ref. 1) waste heat exchanger coolant-inlet temperature is about 6 to 11 K (10° to 20° F) lower than the compressor-inlet temperature. Hence, above compressor-inlet temperatures of about 320 K, the radiator areas in figure 9 are larger than those that could be obtained without the coolant-inlet temperature limit. For example, if the cold-plate inlet temperature were not limited, the lowest specific radiator areas (those at a compressor-inlet temperature of 333 K and a compressor-outlet pressure of 31.0 N/cm^2) would be 4.8 m^2/kWe (52 ft^2/kWe) at a sink temperature of 222 K; 5.5 m^2/kWe (59 ft^2/kWe) at 250 K; and 6.7 m^2/kWe (72 ft^2/kWe) at 278 K.

In radiator-area-limited applications, a user might wish to consider alternate cooling arrangements for the power system's secondary cooling needs.

The three dashed curves on each map in figure 9 are for constant values of power-conversion-module thermal input. The slopes of these curves show the rate of change in power output with radiator area for a fixed-size heat source. The rate of change is the largest near a compressor-inlet temperature of 333 K. As compressor-inlet temperature is reduced, the slope rapidly approaches zero. The design compressor-inlet temperature of 300 K was chosen as a reasonable compromise at a radiator heat-sink temperature of 250 K for increased efficiency at some penalty in radiator area. The operational power output range at a compressor-inlet temperature of 300 K is from 1.5 to 10.5 kilowatts, electric. Net conversion efficiency increases from 0.13 at 1.5 kilowatts to 0.28 at 10.5 kilowatts. At a sink temperature of 250 K, the specific radiator needs decrease from about 20 m^2/kWe (220 ft^2/kWe) at 1.5 kilowatts to about 7.2 m^2/kWe (78 ft^2/kWe) at 10.5 kilowatts.

CONCLUDING REMARKS

Data from the first tests on the 2- to 15-kilowatt space electric power system in a vacuum chamber were compared with analytical predictions of its performance. Because of uncertainties in exact test conditions and incompletely explained performance, comparisons were limited to test results from the second of two sets of identical turbomachinery and the design helium-xenon working gas mixture.

Differences between analytical values and measurements were expressed in percent of the largest measured value for each quantity. The pretest analytical values for gross conversion efficiency and alternator gross power output were higher than the measurements. Differences were no more than +9 percent for conversion efficiency and +6 percent for gross power output. The combination of neglected effects and minor differences between assumed analytical conditions and test conditions were not of major importance. Judgements based on the pretest analysis were valid.

Inclusion of a heat-loss term in a modification of the pretest analysis and minor refinements in the assumed analytical conditions brought the test data and analytical results into closer agreement. The modified analysis correlated gross conversion efficiency and alternator gross power output. Differences were no greater than ±2.5 percent in efficiency and ±2.0 percent in power output. Although the comparisons with test data were limited, the authors believe that the modified analysis can be used to accurately project current power system performance in user application studies. Although these analyses were made specifically for the 2- to 15-kilowatt power system, the methods can be used for other closed Brayton cycle systems.

Lewis Research Center,
National Aeronautics and Space Administration,
Cleveland, Ohio, March 16, 1972,
112-27.

REFERENCES

1. Klann, John L.: Steady-State Analysis of a Brayton Space-Power System. NASA TN D-5673, 1970.
2. Vernon, Richard W.; and Miller, Thomas J.: Experimental Performance of a 2-15 Kilowatt Brayton Power System Using a Mixture of Helium and Xenon. NASA TM X-52936, 1970.

3. Klann, John L.; and Wintucky, William T.: Status of the 2- to 15-kWe Brayton Power System and Potential Gains from Component Improvements. Proceedings of the Intersociety Energy Conversion Engineering Conference. SAE, 1971, pp. 195-201.

4. Valerino, Alfred S.; Macosko, Robert P.; Asadourian, Armen S.; Hecker, Thomas P.; and Kruchowy, Roman: Preliminary Performance of a Brayton-Cycle-Power-System Gas Loop Operating With Krypton Over a Turbine Inlet Temperature Range of 1200° F to 1600° F. NASA TM X-52769, 1970.

5. Nusbaum, William J.; and Kofskey, Milton G.: Cold Performance Evaluation of 4.97-Inch Radial-Inflow Turbine Designed for Single-Shaft Brayton Cycle Space-Power System. NASA TN D-5090, 1969.

6. Weigel, Carl, Jr.; Tysl, Edward R.; and Ball, Calvin L.: Overall Performance in Argon of 4.25-Inch Sweptback-Bladed Centrifugal Compressor. NASA TM X-2129, 1970.

7. Repas, David S.; and Edkin, Richard A.: Performance Characteristics of a 14.3-Kilovolt-Ampere Modified Lundell Alternator for 1200 Hertz Brayton-Cycle Space-Power System. NASA TN D-5405, 1969.

8. Thollot, Pierre A.; Bainbridge, Richard C.; and Nestor, James: Description and Performance of the Electrical Subsystem for a 2- to 15-kWe Brayton Power System. Presented at the AIAA Intersociety Energy Conversion Engineering Conference, Las Vegas, Nev., 1970.

9. Futral, Samuel M.; and Nusbaum, William J.: Effect of Axial Running Clearance on Performance of Two Brayton Cycle Radial Inflow Turbines. NASA TM X-52552, 1969.

10. Wong, Robert Y.; Klassen, Hugh A.; Evans, Robert C.; and Winzig, Charles H.: Preliminary Investigation of a Single-Shaft Brayton Rotating Unit Designed for a 2- to 10-Kilowatt Space Power Generation System. NASA TM X-1869, 1969.

11. Miller, T. J.; Couch, J. P.; and Prok, G. M.: Design and Preliminary Testing of a Brayton Space Radiator Concept. Proceedings of the Intersociety Energy Conversion Engineering Conference. SAE, 1971, pp. 403-408.

NASA-Langley, 1972 —— 3 E-6811